Pure Appl. Chem., Vol. 78, No. 4, pp. 791–811, 2006.
doi:10.1351/pac200678040791

Ring *carbo*-mers: From questionable homoaromaticity to bench aromaticity*

Chunhai Zou, Christine Lepetit, Yannick Coppel, and Remi Chauvin‡

Laboratoire de Chimie de Coordination du CNRS, UPR 8241, 205 Route de Narbonne, 31700, Toulouse Cédex 4, France

Abstract: The title journey is undertaken at the levels of both theory and experiment. Since 1983, homoaromaticity has been shown to play at most a minor role in the stability of Scott's [N]pericyclyne hydrocarbons—the first ring *carbo*-mers of cycloalkanes. This statement has been systematically refined for N = 3–6 by using both classical theoretical tools and newly designed tools based on electron localization function (ELF) analysis. The compatibility of the [5]- and [6]-pericyclyne cores with vertex functionalities was established by the synthesis of 20 oxy (*carbo*-cyclitol) derivatives. The stereoisomeric resolution of two of them has been achieved. Hexaoxy-[6]pericyclynes are actually potential precursors of the *carbo*-benzenes. Criteria based on density functional theory (DFT) calculations (magnetic, energetic, structural/"electronic") show that the aromaticity of *carbo*-[N]annulenic species is comparable to that of their parent molecule. This has been challenged by the synthesis of several novel *carbo*-benzenic molecules with various substitution patterns. The theory–experiment interplay is pursued by considering ring *carbo*-mers of other conjugated ring systems such as radialenes. The second *carbo*-mers (butadiyndiyl-expanded rings) of [3]radialene and benzene are also envisioned. Hexaphenyl-*carbo*$_2$-benzene has been observed by ^{1}H NMR and UV–vis spectroscopy.

Keywords: *carbo*-mers; homoaromaticity; bench aromaticity; pericyclynes; *carbo*-cyclitol; DFT; radialenes.

INTRODUCTION

Scientific activity takes place at three levels: the appraisal of phenomena, the translation of them into concepts, and the endeavor of bringing the latter into consistent theoretical frames through explicit quantitative definitions. Some of these concepts are "narrow" in their scope, and others are "wide". Among open challenges in chemistry, narrow concepts can be illustrated by the Kohn–Hohenberg universal functional [1], whereas wide concepts can be exemplified by the notion of atoms inside molecules and atomic charges [2], molecular chirality [3], and, of course, aromaticity [4]. Just like its companions, aromaticity is still a fuzzy concept and should remain so forever. Its fuzziness is indeed intrinsic for historical reasons, and the associated "mystery" is the intellectual driving force of the search for concealed correlations between aromaticity criteria. In an attempt to clarify various notions evoked within the framework of the aromaticity theory, a synoptic rationale is proposed in Table 1. Katritsky's principal component analysis (PCA) [5] first proposed a dichotomy of the aromaticity con-

*Paper based on a presentation at the 11th International Symposium on Novel Aromatic Compounds (ISNA-11), St. John's, Newfoundland, Canada, 14–18 August 2005. Other presentations are published in this issue, pp. 685–888.

‡Corresponding author

cept depending on the molecular context: isolated (static) or embedded into an external magnetic field (dynamic). These contexts cover two (structural and energetic) and one (magnetic) of the classical aromaticity criteria, respectively. Each criterion is actually associated with one observable, for which several indices have been proposed. For example, the average C–C bond length d_{av} and the root mean square deviation σ(d), which are respectively proportional to Krygowki's energetic (EN) and geometric (GEO) parameters, proved to be relevant indices of structural aromaticity [6]. Likewise, resonance/aromatic stabilization energies (REs/ASEs) [4] and nucleus independent chemical shifts (NICSs) [7] are currently used to measure energetic and magnetic aromaticity, respectively. Nonetheless, each criterion corresponds to a physico-topographical origin: While ring currents and (π) molecular orbitals (MOs) stand at the origin of the magnetic and energetic criteria, respectively, electron density clearly stands at the origin of the structural criterion. It is proposed that a mathematical tool is adapted to quantify and visualize the cyclic delocalization component from each topography. While ring current mapping or stagnation graphs are the tools of choice for the magnetic criterion [8], orbital localization procedures might be those for the energetic criterion [9]. The electron localization function (ELF) of the electron density [10] can be used in various manners to quantify electron delocalization and structural aromaticity (weighting of resonance forms from partition maps, critical iso-ELF values of the bifurcation trees, ELF Hückel numbers (EHNs): see below). While structural and energetic aromaticity criteria are intrinsically correlated through the Hückel rule, static and dynamic contexts have no reason to be systematically correlated, just as a ponctual value (at $B_{ext} = 0$) does not define a function over further B_{ext} values. A universal correlation must depend on nonstatic molecular parameters, but static and dynamic criteria can be incidentally correlated over a sufficiently homogeneous set of molecules for which such parameters remain within a restricted range. This was proposed, for example, by Schleyer et al. for a set of five-membered unsaturated rings [11].

Table 1 Synoptic relationships between notions and tools currently associated with the aromaticity concept. The "visualization-analysis tool" entry is proposed as a tentative harmonization.

Separation	Katritsky's PCA analysis: "the aromaticity concept is two-dimensional"		
Context	Static		Dynamic
Criterion	Structural <—> energetic		Magnetic
Observables	Bond distances	Reaction enthalpies	Magnetic susceptibilities, NMR
Indices	Symmetry, HOMA, EN, GEO (s(d)),…	Hückel rules, ASEs, REs,…	Magnetic exaltation/anisotropy, nuclear (de)shielding, NICS,…
Origin	Electron density	Canonic orbitals	Ring currents
Visualization-analysis tool?	ELF analysis (Silvi–Savin, Santos…)	Localization procedures (Pipek–Mezey,…)	CTOCD-DZ maps, stagnation graphs (Fowler, Lazzeretti,…)
Correlation	Schleyer's suggestion: "classical and magnetic concepts may not be orthogonal"		

Another tentative way to "homogenize" a set of molecules is the axiomatic definition of the *carbo*-meric relationship, which has been devised from a comparative standpoint [12]: Any property of a given parent molecular system *qualitatively* exists in its *carbo*-mer. Most of the molecular model features, but the "carbon content" and size, are indeed preserved in *carbo*-mers: original atom connectivity, valence shell electron pair repulsion (VSEPR) shape and/or symmetry, Cahn–Ingold–Prelog (CIP) configurations of stereogenic centers, π-resonance,… If the parent molecule is cyclically conjugated, aromaticity is the chief property underlying many others (stability, (hyper)polarizability, hapticity,…). Since a proven chemical route to "aromatic" *carbo*-mers (e.g., *carbo*-[N]annulenes) proceeds through aromatization of functional ring *carbo*-mers of the corresponding saturated ring, comparison of the

homo-conjugated *carbo*-meric precursor (e.g., [N]pericyclynes) with the corresponding saturated parent molecules (e.g., N-membered cycloalkanes) is a prerequisite. The possibility of π-homoaromaticity in pericyclynes does not exist in the parent cycloalkanes, and it has been proven that homoaromaticity has no incidence on the stability of the nonfunctional [5]pericyclynes $C_{15}H_{10}$ [13]. The first task was, therefore, to investigate the compatibility of oxy substituents with the pericyclynic rings. This was undertaken at both experimental and theoretical levels.

RING *CARBO*-MERS OF CYCLOALKANES: [N]PERICYCLYNES

The term "pericyclyne" was coined by Scott et al. in the mid-1980s as they reported on the synthesis of the first permethylated representatives, which turned out to be remarkably stable [14]. Unsubstituted [5]pericyclyne was later calculated to be planar at the B3LYP/6-31G* level, but it was shown to be not homoaromatic on the basis of classical aromaticity criteria [13]. At a comparable level of calculation, we performed the ELF analysis of [N]pericyclynes, N = 3–6 to weight the localized and cyclically delocalized Lewis forms (Fig. 1). Electron homodelocalization was found negligible for the higher members of the series, but it reaches 8 % in [3]pericyclyne [15].

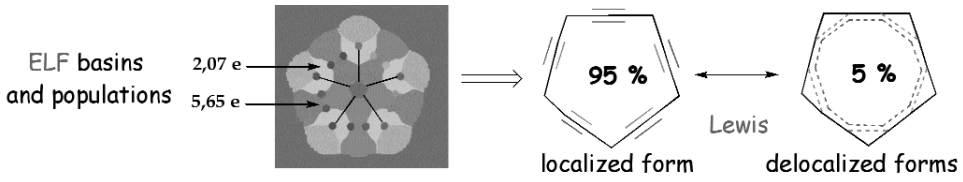

Fig. 1 ELF weighting of resonance forms in unsubstituted [5]pericyclyne [15].

Functional pericyclynes

More than 20 N-oxy-[N]pericyclynes (N = 5, 6) have been synthesized in 7–20 steps via various [(3N–n)+n] ring formation steps consisting in a double nucleophilic attack of a (3N–n)-carbon ω-diacetylide to a n-carbon ω-dicarbonyl alkyne (Fig. 2) [16,17]. These molecules can be regarded as derivatives of *carbo*-[N]cyclitols (N = 5,6), for which many substitution patterns have been exemplified: the vertices can be sp^3-secondary (C(H)OR, R = H, Me), sp^3-tertiary (C(R')OR, R' = Ph, 4-An, 4-py, C≡C–SiR"$_3$), sp^3-masked carbonyls (ketal), sp^2-carbonyls, or sp^3-heteroatomic (P(O)Ph, $SiPh_2$). Most of them were obtained as mixtures of stereoisomers. Nevertheless, the most symmetrical representatives could be resolved through semipreparative high-performance liquid chromatography (HPLC) or spontaneous crystallization.

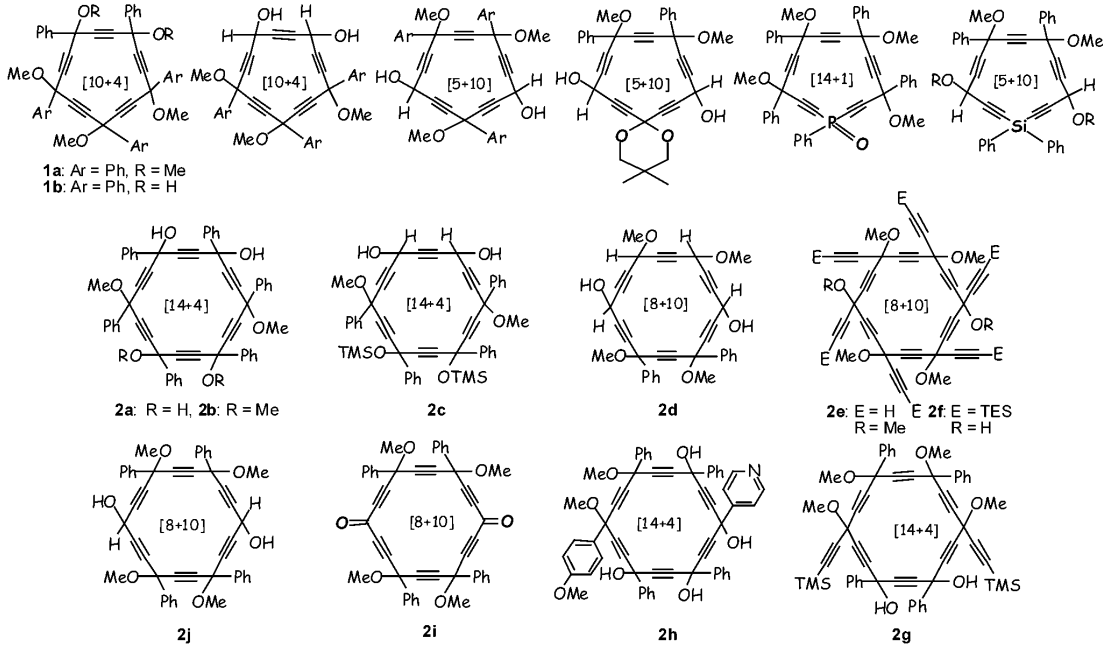

Fig. 2 Synthesized [5] and [6]pericyclynes. The ring formation step is indicated by the [(N–n)+n] symbol, $N = 15$, 18.

For example, pentaphenyl-*carbo*-[5]cyclitol pentamethyl ether **1a** was prepared in two steps from a statistical mixture of the three stereoisomers of tetrayne **3** (Fig. 3) [16]. The intermediate diol **1b** displayed the expected number (26) of methoxy ^{1}H NMR signals for a mixture of the 10 possible diastereoisomers. After increasing the symmetry by methylation, the pentaether **1a** displayed the expected number (10) of methoxy ^{1}H NMR signals for a mixture of the four possible diastereoisomers. Starting from the major stereoisomer of **3** (resolved by semipreparative HPLC), the expected remaining 3 stereoisomers of **1a** were statistically obtained in an oily mixture. Semipreparative HPLC allowed for isolating single stereoisomers of **1a** as white crystalline solids (Fig. 3). Since monocrystals of these compounds were not suitable for X-ray diffraction analysis, the corresponding unsubstituted *carbo*-[5]cyclitols were calculated at the B3PW91/6-31G** level of theory. The optimized structures are slightly twisted, and the endocyclic bond lengths do not exhibit significant difference as compared to those found in the density functional theory (DFT)-optimized or X-ray crystal structures of nonfunctional Scott's [5]pericyclynes [14]. These results show that oxy substituents are fully compatible with the features of the "naked" [5]pericyclyne core.

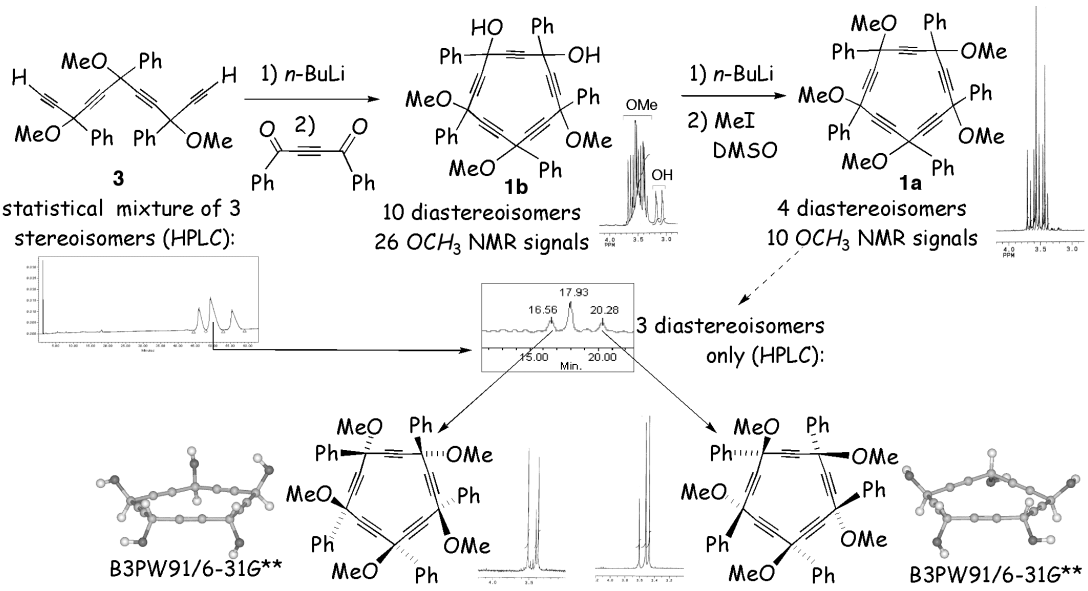

Fig. 3 Synthesis, stereochemical resolution, and DFT calculations of hexaoxy-[5]pericyclynes [16].

In the [6]pericyclyne series, the hexamethylether of hexaethynyl-*carbo*-[6]cyclitol (**2e**) was recently prepared. A single stereoisomer of **2e** was isolated by spontaneous crystallization, for which an X-ray diffraction analysis revealed a chair structure of D_{3d} symmetry, where the ethynyl substituents occupy axial positions, while the methoxy substituents occupy equatorial positions (Fig. 4) [18].

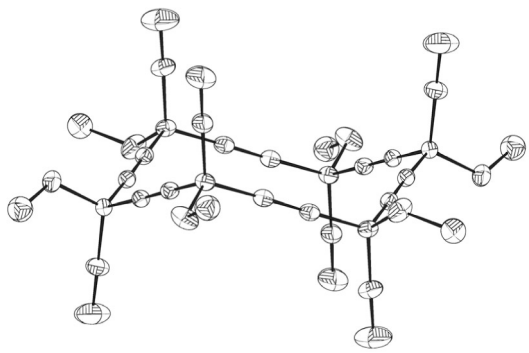

Fig. 4 X-ray crystal structure of the all-*trans* stereoisomer of hexaethynyl-hexamethoxy-[6]pericyclyne **2e** [18].

Carbo-benzenes

Mixtures of stereoisomeric functional hexaoxy-[6]pericyclynes were treated with the reducing $SnCl_2$/HCl system. Though poorly selective, the reaction afforded several *carbo*-benzene derivatives in 5–20 % yield (Fig. 5) [19]. Hexaphenyl-*carbo*-benzene, $C_{18}Ph_6$ (**4**), previously prepared by Ueda, Kuwatani et al. in 15 steps [20], was thus obtained in 10 steps through either precursors **2a** or **2b** [19]. Another hexaaryl-*carbo*-benzene, the *p*-(pyridyl, anisyl)-disubstituted tetraphenyl-*carbo*-benzene **5**, was obtained from the totally disymmetric [6]pericyclyne **2h**. It has been characterized by mass spectrometry (MALDI-TOF: [M–H]+ = 709.9) and UV–vis spectroscopy [λ_{max} = 476 nm (ε = 16 300), 522 nm (sh, ε = 4900)] [19]. This push–pull chromophore was also investigated for its possible second-

order NLO properties. Its quadratic hyperpolarizability estimated by EFISH measurement in dioxane ($|\beta_{1.907\mu m}|$ = 66 10^{-30} cm^5 esu^{-1}) [21] is in qualitative agreement with the corresponding Zindo-calculated hyperpolarizability in vacuum ($\beta_{1.907\mu m}$ = 36 10^{-30} cm^5 esu^{-1}) [22].

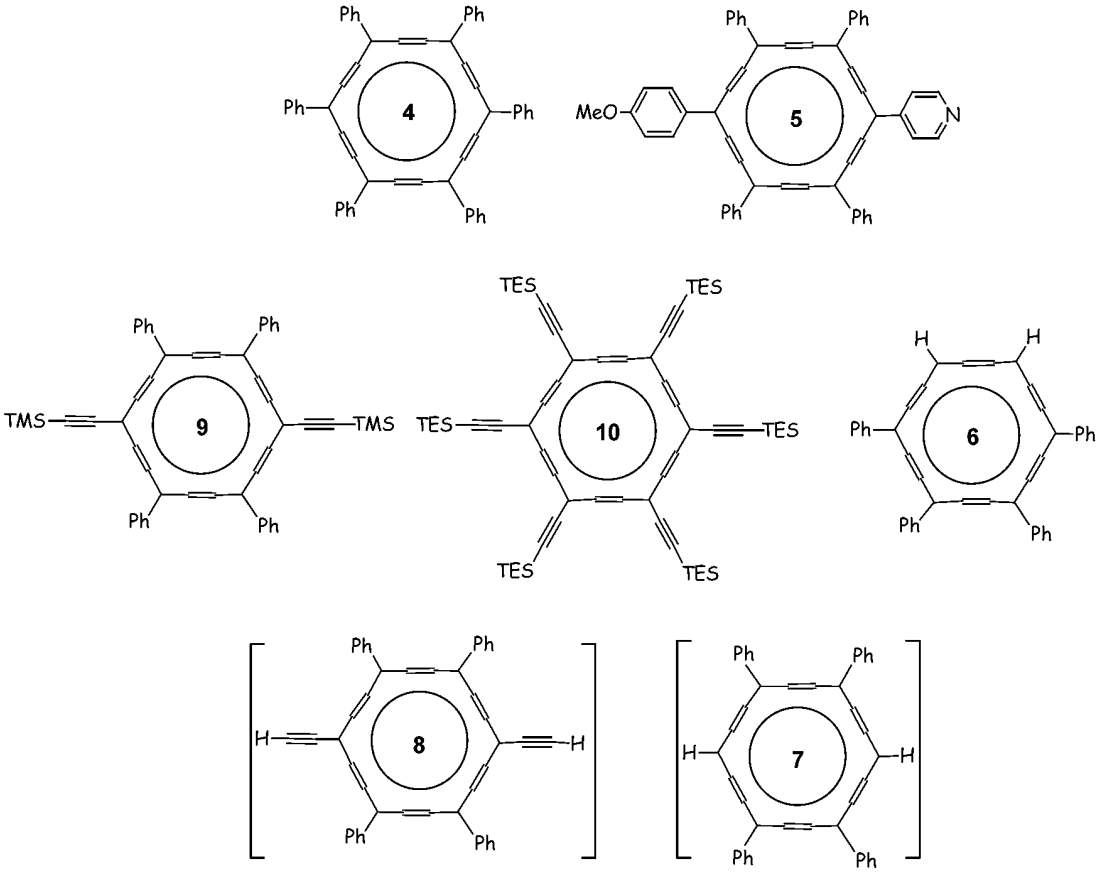

Fig. 5 Synthesized *carbo*-benzene derivatives **4–6**, **9–10**, with various substitution patterns. Derivatives **7** and **8** were not isolated, but detected through their peculiar, strongly deshielded ^{1}H NMR signals [19].

Tetraphenyl-*carbo*-benzene, $C_{18}Ph_4H_2$ (**6**) without substituent in ortho positions and with reduced potential radial conjugation, was isolated from **2c** under controlled conditions: Its stability, ^{1}H NMR spectrum, and X-ray crystal structure (Fig. 6) confirm its theoretically predicted aromaticity [19]. A very good agreement was indeed found between the experimental and calculated structures (B3PW91/6-31G** level) of **6** [23]. Tilting of the phenyl substituents with respect to the *carbo*-benzenic ring originates from van der Waals repulsions between phenyl *o*-H atoms. Similarly, the experimental and calculated ^{1}H NMR spectra are in qualitative agreement. These results show that the selected DFT level of calculation (based on a hybrid functional) is well suited for this family of compounds. The D_{6h} symmetry of the C_{18} ring, and (within the recognized limits of significance) the large negative NICS value calculated at its geometric center (–14.8 ppm at the B3LYP/6-31+G** level) are indicative of structural aromaticity and magnetic aromaticity, respectively.

The para isomer **7** of tetraphenyl-*carbo*-benzene, as well as the *p*-diethynyl-tetraphenyl-*carbo*-benzene **8** (Fig. 5) could not be isolated in the pure state, but their ^{1}H NMR spectra, identified through chemical and theoretical correlations, revealed a strong ring current effect on the corresponding exter-

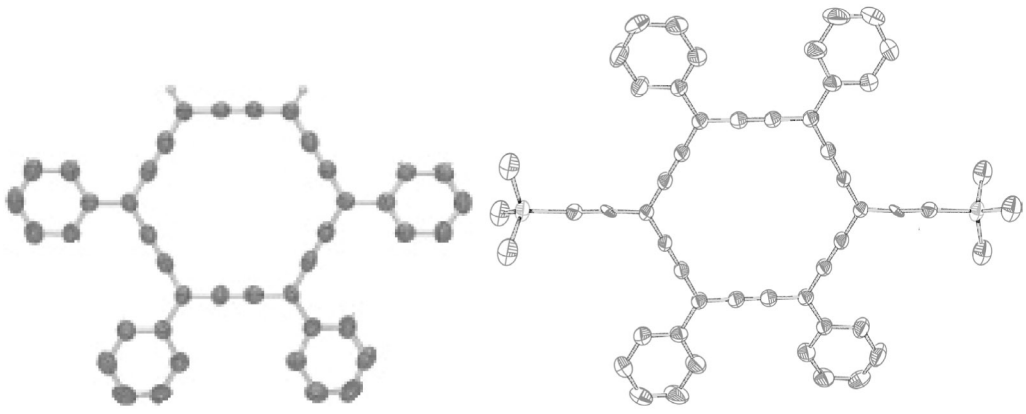

Fig. 6 X-ray crystal structures of tetraphenyl-*carbo*-benzene derivatives **6** (left) and **9** (right) (Fig. 5) [19].

nal protons. By contrast, the trimethylsilyl (TMS)-protected version of **8** (**9**) was obtained by aromatization of **2g** and fully characterized, including by its X-ray crystal structure (Fig. 6) [19]. Very recently, the hexa(triethylsilylethynyl)-*carbo*-benzene **10**, *without any aromatic substituent*, also proved to be stable: It is a protected version of the total *carbo*-mer of benzene $C_{18}(C{\equiv}CH)_6$ [18].

In Table 2, the aromaticity of various *carbo*-benzene derivatives is compared through calculated structural (d_{av}, $\sigma(d)$) and magnetic (NICS(0)) indices. Both criteria indicate that aromaticity decreases upon substitution of the C_{18} ring by phenyl or ethynyl groups. Comparison of the experimental ^1H chemical shifts of the external protons of **4** and **6** confirms this trend: the effect of the ring current is indeed slightly weaker in the hexaphenyl derivative (**4**) than in the tetraphenyl one (**6**).

Table 2 Comparison of structural and magnetic aromaticity of various *carbo*-benzene derivatives. Geometries are calculated at the B3PW91/6-31G** level, central NICSs are calculated at the HF/6-31+G* level. Experimental ^1H chemical shifts (in brackets) were measured in $CDCl_3$ solution.

	C_6H_6	$C_{18}H_6$	*o*-$C_{18}Ph_4H_2$ **6** (exp.)	$C_{18}Ph_6$ **4** (exp.)	$C_{18}(C{\equiv}CH)_6$
d_{av} (Å)	1.394	1.326	1.329 (1.33)	1.332 (1.33)	1.332
$\sigma(d)$ (Å)	0	0.061	0.066 (0.066)	0.068 (0.066)	0.070
NICS (ppm)	–9.7	–19.7	–16.8	–15.5	–17.8
δ_{1H} (ppm)	(7.27)	–	(9.70, 9.55, 8.05, 7.77)	(9.45, 7.99, 7.72)	–

The *carbo*-meric comparison of the aromaticity of benzene and *carbo*-benzene is now envisioned through the following three criteria.

- Relative magnetic aromaticity of benzene and *carbo*-benzene. Experimental (magnetic deshielding of peripheral protons), and calculated (NICS) indices clearly indicate that the *carbo*-benzene ring is magnetically more aromatic than benzene (Table 2). Ring current analysis by Fowler et al. at the CTOCD-DZ-CHF/6-31G** level also revealed strong total ($\sigma+\pi$) and π diamagnetic circulations, confirming the strong magnetic aromaticity of *carbo*-benzene [24].
- Relative structural aromaticity of benzene and *carbo*-benzene. The available structural indices d_{av} and $\sigma(d)$ cannot be directly compared for benzene and *carbo*-benzene. A suitable general measure was therefore required. As proposed in the introduction, electron density is at the origin of static structural aromaticity, and ELF is *a priori* a relevant analytic tool (Table 1). Recently, a new aromaticity scale, based on the separation of the ELF into σ and π contributions, was introduced by Santos et al. [25]. The partial ELF (σ or π) value for which the separation of the localization domains of the fully unsaturated ring occurs, is chosen as the (σ or π) aromaticity index. Benzene

($ELF_\pi = 0.91$) lies quite high in this aromaticity scale ranging from zero to one ($ELF_\pi \approx 1.00$ is attained for the cyclopropenyl cation). *Carbo*-benzene, with $ELF_{\pi z} = 0.86$, appears to be slightly less aromatic than its parent molecule (Fig. 7). Thus, while *carbo*-benzene is magnetically more aromatic than benzene, the converse holds for structural aromaticity.

- Relative energetic aromaticity of benzene and *carbo*-benzene. Several indices of energetic aromaticity such as REs or ASEs have been defined in the literature for benzene (containing sp^2 carbons only) [4]. These schemes were generalized to *carbo*-benzene (containing both sp^2 and sp carbons) [23].

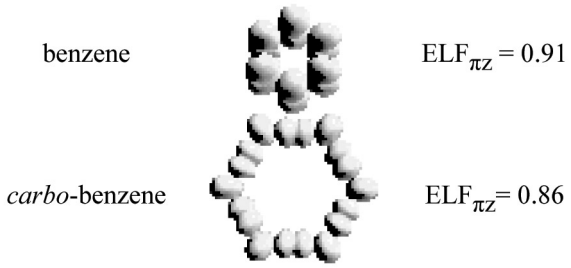

Fig. 7 ELF_π isosurfaces for benzene and *carbo*-benzene at critical ELF_π values where disconnection of the endocyclic localization domains occurs (B3PW91/6-31G**).

The Dewar–Mulliken–Parr RE [26] compares the aromatic molecule with one of its Kekulè form at the same level of calculation. It therefore estimates the stabilization resulting from the (cyclic) electron delocalization. Two sets of values, calculated at the B3PW91/6-31G** level, are given in Fig. 8 for benzene and its ring *carbo*-mer. They correspond to different approximations for the fictitious Kekulè form of D_{3h} symmetry with the *same cyclic conjugation potential* as in the real ring of D_{6h} symmetry. For example, in the case of benzene, the lengths of the double and single C–C bonds of the Kekulè form may be respectively extracted from ethylene and ethane, or from all-*trans* hexatriene and hexadiene. As expected, the calculated stabilization is strongly reduced when the bond lengths are extracted from the longer acyclic fragments. Both sets of RE values suggest that *carbo*-benzene is slightly less (cyclically) delocalized than benzene.

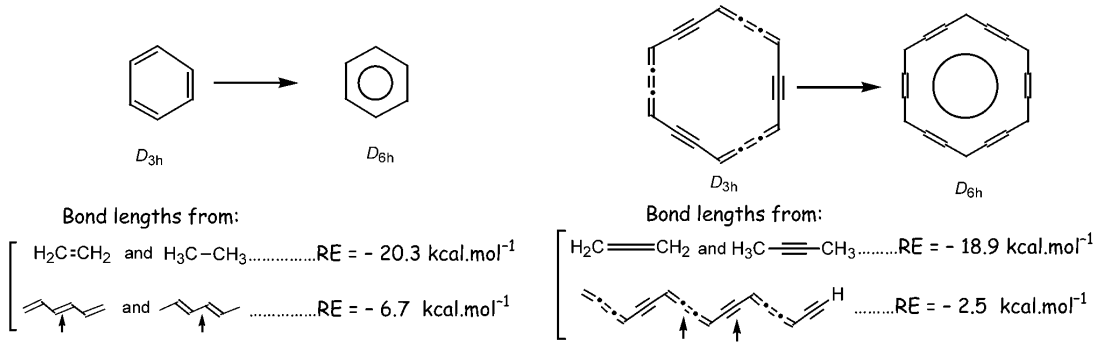

Fig. 8 Dewar–Mulliken–Parr REs for benzene and its ring *carbo*-mer.

However, the D_{3h} structures are as cyclic as the equilibrium benzene structure, and the Dewar–Mulliken–Parr stabilization energy surely underestimates the stabilization resulting from the *cyclicity* of the electron delocalization. Several cyclizing ASE schemes have been introduced in the literature to estimate the corresponding energetic *topological* aromaticity. Their relevance increases with the conservation of local atomic environments (bond types, hybridization state, conjugation extent). They are illustrated for benzene by reference to acyclic fragments ranging from ethylene to 1,3,5-hexatriene (Fig. 9). In the isogyric scheme, H_2 molecules, and thus troublesome H–H bonds, are required to equilibrate the reaction scheme. In the isodesmic scheme introduced by Hehre et al. [27], both sides of the equation include the same number of bonds of given order between elements. The homodesmotic scheme [28], involving the same number of bonds of given order between elements of given hybridization states on each side of the equation, provides a better approach to the cyclicity stabilization value. The hyper-homodesmotic scheme involving the same number of bonds of given substitution pattern on each side of the equation [29] is supposed to give an even more reliable estimate of the energetic aromaticity. If n denotes the ratio to 3 (i.e., the number of formal double bonds in benzene) of the number of double bonds in the left-hand side alkene, the ASE schemes (Fig. 9) can be regarded as the first representatives (for n = 1/3, 2/3, 1, respectively), of a general class of cyclizing "n-isoconjodesmic" reactions. The conservation of the bond types and of the delocalization (spatial) extent increases with n (the latter extent is infinite in the fully unsaturated ring). Along this line, the two Dewar–Mulliken–Parr schemes proposed above for benzene and *carbo*-benzene (Fig. 8) could be regarded as examples (for n = 1/3, 1) of noncyclizing "n-isoconjodesmic" schemes.

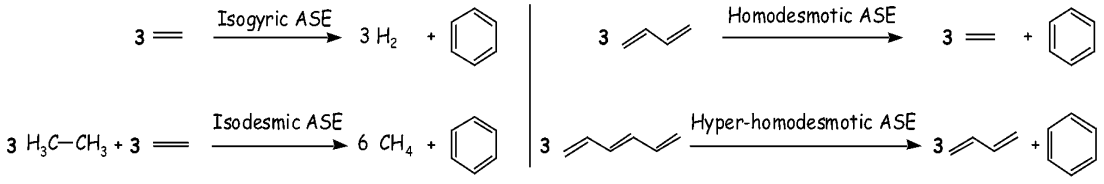

Fig. 9 Schemes of ASEs specifically measuring the effect of the cyclicity of the π-electron delocalization for benzene.

The homodesmotic scheme affords $\Delta E(C_6H_6)$ = –23.5 kcal mol^{-1} at the B3PW91/6-31G** level (Fig. 10), which is close to the value of –19.5 kcal mol^{-1} reported by Schleyer et al. at a comparable level of calculation (B3LYP/6-31G*) [30]. The corresponding equation for *carbo*-benzene is defined by replacing each reactant and product for its skeleton *carbo*-mer (Fig. 10). The ASE calculated at the B3PW91/6-31G** level is found to be merely 40 % less negative than for benzene [$\Delta E(C_{18}H_6)$ = –14.1 kcal mol^{-1}]. *Carbo*-benzene is, therefore, less energetically aromatic than benzene.

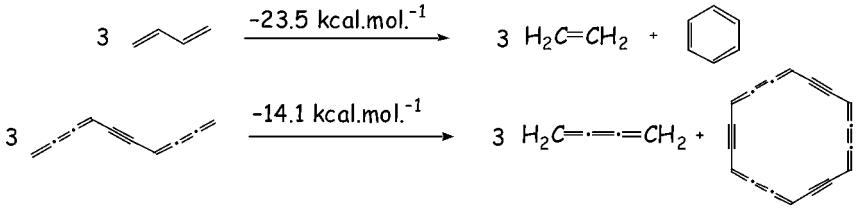

Fig. 10 Homodesmotic ASEs for benzene and *carbo*-benzene.

The isogyric equations of Fig. 11 directly compare the C_6 (resp. C_{18}) π-electron ring with the same, but acyclic, C_6 (resp. C_{18}) π-electron chain. Since a ring closure turns on the possibility of a ring current, and since the diatropicity of aromatic molecules is mainly due to their π-electrons, this isogyric equation is expected to be closely related to the magnetic criterion of aromaticity. At the B3PW91/6-31G** level, the isogyric ASE is equal to –17.9 kcal mol^{-1} for benzene, and to –11.2 kcal mol^{-1} for *carbo*-benzene. It is, however, noteworthy that the acyclic structures are taken in their most stable all-*trans* conformation, and that this ASE scheme thus underestimates the pure topological cyclicity effect.

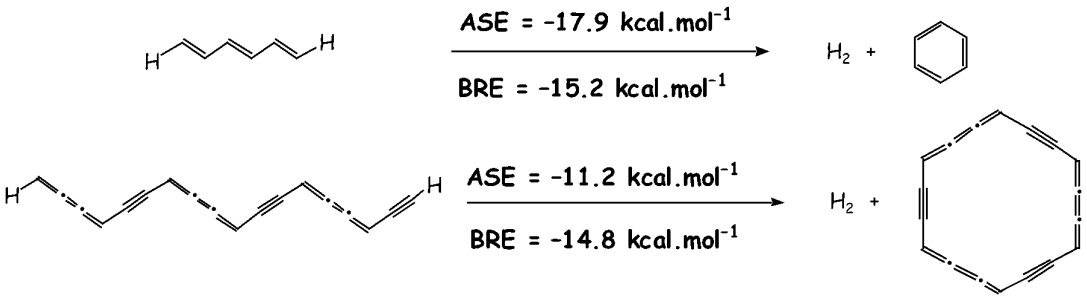

Fig. 11 "Ring-closing" isogyric equations defining an ASE and the Breslow resonance energy (BRE) of benzene and *carbo*-benzene.

In accordance with Shaik's theory [31], the isogyric ASEs of Fig. 11 explicitly refer to both the π- and σ-electron systems. However, the σ-electrons of the H–H bond on the right-hand side are isolated, while the "same" electrons in the C–H bonds on the left-hand side are "conjugated" with further C–C and C–H bonds. The devised merit of this isogyric scheme (ring closure = turn on) must, therefore, be restored by considering the π-electron system separately. This can be achieved within the framework of the topological Hückel molecular orbital (HMO) theory, the semi-empirical parameter (β) of the benzene molecule serving to define a fictitious reference 1,3,5-hexatriene π-system. Within the HMO framework, Breslow defined the resonance energy of benzene as: E_π(benzene) – E_π(1,3,5-hexatriene) [32]. This definition generalized to any [N]annulenic species reads: BRE = $2\beta[\sum n_k \cos(2k\pi/N) - \sum n'_k \cos(k\pi/(N+1)]$, where β is an average C–C resonance integral; n_k and n'_k are the numbers of electrons occupying the k^{th} π-MO in the ground states of the [N]annulenic and corresponding N-polyenic species, respectively ($\sum n_k = \sum n'_k = N - q$, where q is the total charge; if $q = 0$, the first sum, namely the annulene π-energy, is equal to: $4\beta/\sin(\pi/N)$ [33]). This formula also holds for any dehydro[N]annulene as soon as the sp–sp and sp–sp^2 resonance integrals can be averaged. This was found to be possible for *carbo*-annulenes, since DFT and Hartree–Fock (HF) π-MO levels accurately vary as $\cos(2k\pi/N)$ [34]. It was also incidentally observed that the extracted β values vary with the annulene size as: $\beta = \beta_\infty N/(N+2)$, where β_∞ = cste. Consequently, the "spectroscopic" proportionality factors β can be renormalized to "thermochemical" values (by setting β_∞ = –20 kcal mol^{-1}), thus allowing for a direct comparison of the BRE with the ASE. The cases $N = 6$ and $N = 18$, finally lead to BRE(C_6H_6) = –15.2 kcal mol^{-1} and BRE($C_{18}H_6$) = –14.8 kcal mol^{-1}, respectively. These results confirm that *carbo*-benzene is slightly less energetically aromatic than benzene.

The relative energetic and structural aromaticities of benzene and *carbo*-benzene, as respectively measured by the $ELF_{\pi z}$ and RE/ASE indices, are thus fully consistent. They are indeed supposed to reveal the same kind of aromaticity in the static (classical) context (Table 1).

Carbo-[N]annulenic species, $N \neq 6$

Beyond *carbo*-benzene, the aromaticity of a complete set of *carbo*-[N]annulenic species $[(C_3H)_N]^q$ has been addressed in their singlet spin state for $(N, q) = (3, -1)$, $(4, 0)$, $(5, +1)$, and in their triplet state for $(N, q) = (4, 0)$. Figure 12 compares various aromaticity measures of [N]annulenes and their ring *carbo*-mers ($N = 3$–6) from optimized geometries at the B3PW91/6-31G** level [34,35]. The experimentally unknown *carbo*-cyclopentadienyl cation [16b] possesses virtually the same NICS and Breslow resonance energy (BRE) values as *carbo*-benzene. The σ(d) value of the ring is also indicative of a similar structural aromaticity for both molecules. The BRE of singlet *carbo*-cyclobutadiene, though negative, is three times smaller (–5.8 kcal mol^{-1}) than it is for 4*n*+2-aromatic annulenic and *carbo*-annulenic species, and its central NICS value (+53.8 ppm) reveals a strong paratropic ring current. In contrast, triplet *carbo*-cyclobutadiene possesses all the features of a totally aromatic molecule. Finally, the *carbo*-cyclopropenyl anion appears strongly aromatic with the same NICS and BRE values as its parent cyclopropenyl cation. All these results are in qualitative agreement with the Hückel rule for the π_z-electron system. It was also confirmed that the in-plane π_{xy}-electron systems play a minor role.

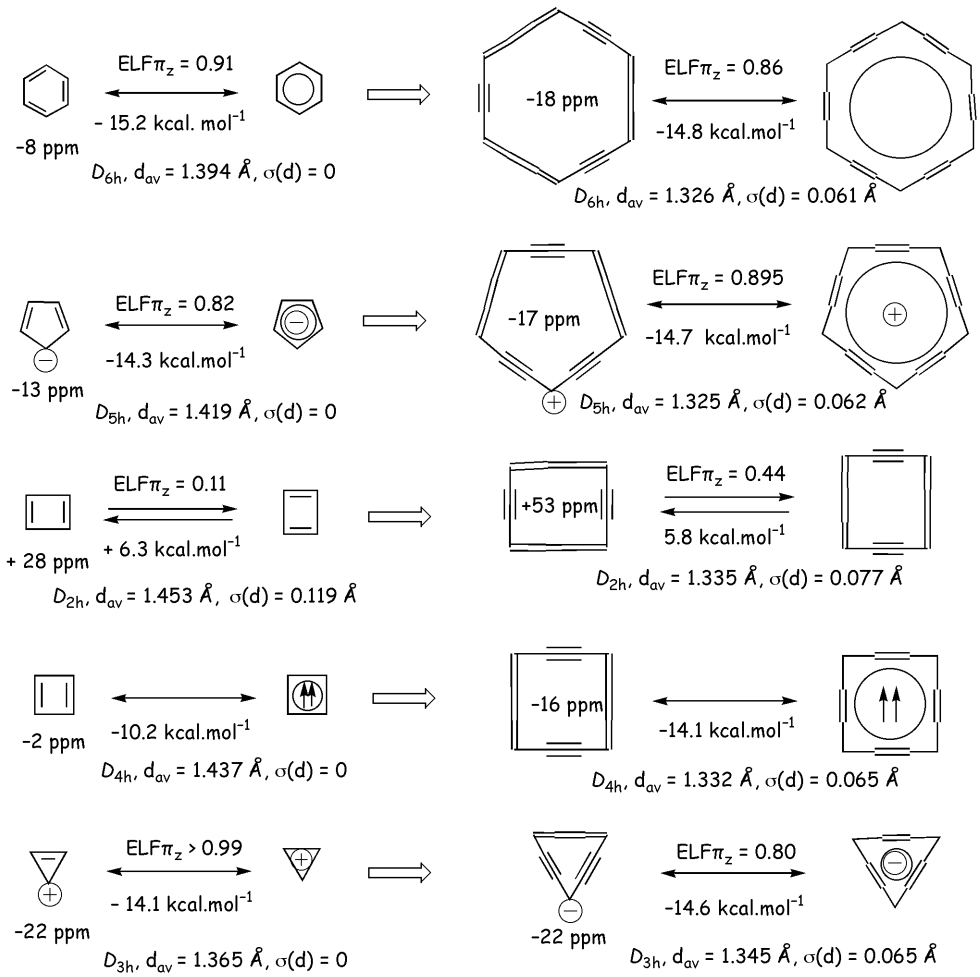

Fig. 12 Aromaticity indices for the first [N]annulenes and their ring *carbo*-mers ($N = 3$–6) in their optimized geometries at the B3PW91/6-31G** level. Magnetic shieldings in ppm correspond to NICS(0) values (GIAO formalism at the B3LYP/6-31+G* level). Energies in kcal mol^{-1} above the arrows correspond to BREs (see text).

Carbo$_k$-[N]radialenes: Aromaticity and electron affinity

The starting point of this study was the experimental observation by Diederich et al. that hexakis(trimethylsilyl) perethynyl derivatives of doubly expanded [4]- and [6]radialenes possess low reduction potentials [36]. An enhanced aromaticity was therefore envisioned for the anions. The geometry and the central NICS of [*carbo*$_k$-[3]radialenes]^q (k = 0, 1, 2, q = 0, –1, –2) in their singlet or doublet spin state were calculated at the B3PW91/6-31G** and B3PW91/6-31+G** level, respectively (Fig. 13) [37]. The rings of all structures were found to be planar with a symmetry close to D_{3h}. The central NICS values become more negative upon reduction, except for the mono-anionic *carbo*-[3]radialene (NICS = +4.0 ppm), which also displays a reduced C_{2v} symmetry. While expanded [3]radialenes are known [38], it is only very recently that a *carbo*-[3]radialene, the hexamethyl derivative, could be experimentally isolated by Tykwinski et al. [39]. Complete structural/electrochemical analysis might thus confirm or qualify the theoretically predicted peculiar behavior of this molecule. It is noteworthy that peripheral hexa-ethynyl substitution of the *carbo*-[3]radialene core (previously studied by Schaeffer III et al. at the HF level [40]), has been predicted to restore the aromatic character of the mono-anion [37].

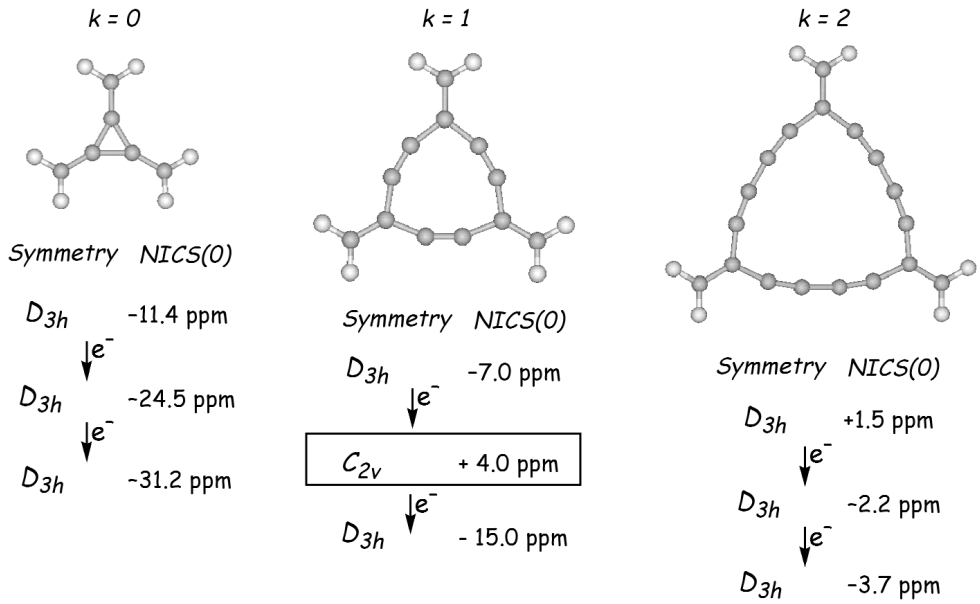

Fig. 13 Variation of symmetry and NICS(0) values vs. reduction of *carbo*$_k$-[3]radialenes (k = 0, 1, 2).

In the *carbo*$_2$-[3]radialenic series, the enhanced aromaticity of the anions and dianions is correlated with the low experimental reduction potentials of the neutral species.

The ELF-weighting of the resonance forms of *carbo*$_k$-[3]radialenic species is consistent with atom-in-molecule (AIM) atomic charges and spin densities. It was used to define a formal average number of endocyclic paired π_z-electrons, the EHN. It was incidentally observed that the closer to a 4m+2 integer the EHN value, the more negative the NICS value. Indeed, from the ELF populations, [3]radialene may be described by two resonance forms (Fig. 14), the major one (60 %) with all-exocyclic π_z-electron pairs, and the minor form accounting for some endocyclic delocalization of π_z electrons. The unexpectedly high weight of the latter form may be partly consistent with the negative NICS(0) value, and with other assessments about the energetic aromaticity of [3]radialene [41]. Upon reduction, the "aromatic" radical forms become the leading ones, in agreement with the still more negative central NICS value: The EHN indeed increases from 0.8 in the neutral [3]radialene to 1.3 in its mono-anion.

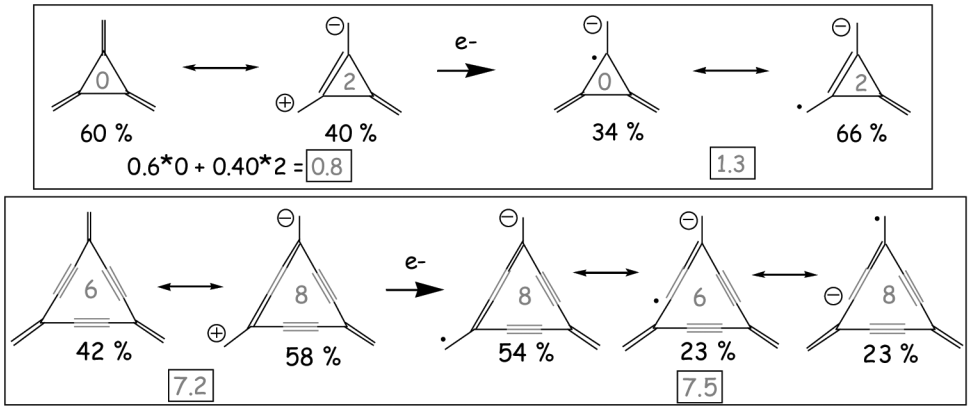

Fig. 14 Definition and evolution of the EHN after monoreduction of radiacycles.

Likewise, upon mono-reduction of *carbo*-[3]radialene, the EHN increases from 7.2 to 7.5, drawing nearer to 8, the integral occupation number of the π_z-MOs for a formally antiaromatic compound: this is in agreement with the corresponding algebraic increase of NICS up to a positive value (+4.0 ppm).

These qualitative illustrations of the heuristic relevance of the EHN are supported by a systematical correlation between EHN, NICS, and σ(d) over a large set of *carbo*$_k$-radialenic species [37]. It must be stressed that for closed π-electron ring systems (e.g., annulenes and their *carbo*-mers), the EHN is strictly equal to the integral orbital Hückel number; it can, however, be relevant not only for radially conjugated systems like *carbo*$_k$-radialenes, but also for condensed polycyclic systems. It has been recently used to consistently analyze the aromaticity of *carbo*-[3]oxocarbon and one of its tetracyclic tricyclopropabenzenic valence isomers [42].

Ring *carbo*-mers of second generation: *Carbo*$_2$-benzene and its hexaphenyl derivative

The second generation of ring *carbo*-mers is more documented through many examples of expanded pericyclynes in the hydrocarbon [43] and functional [44,45] series. Second ring *carbo*-mers of radialenes are also known [46], and were studied at the theoretical level (see above). The second *carbo*-merization process is here applied to the benzene ring. Preliminary DFT calculations first showed that unsubstituted *carbo*$_2$-benzene is magnetically and structurally as aromatic as *carbo*-benzene. These results prompted us to undertake an experimental realization (Fig. 15).

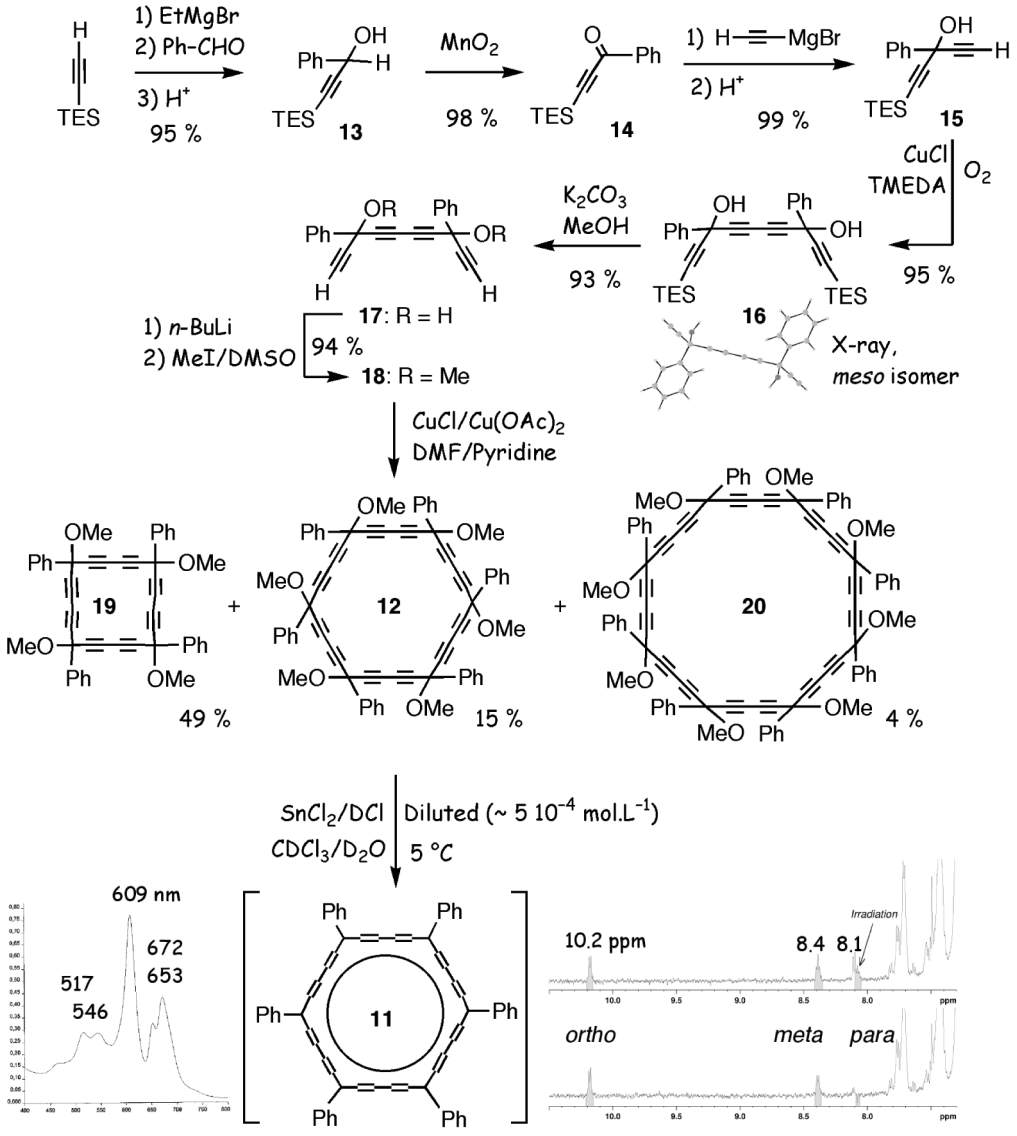

Fig. 15 Synthesis of expanded hexaphenyl-hexamethoxy-[6]pericyclyne, and its subsequent conversion to hexaphenyl *carbo*$_2$-benzene as observed in situ by ^{1}H NMR and UV–vis spectroscopy.

Hexaphenyl-*carbo*$_2$-benzene **11** was targeted through reductive aromatization of the expanded hexaoxy-[6]pericyclyne precursor **12**. The latter could be obtained in seven steps by sequential oxidative couplings of terminal alkynes through the intermediates **13**–**18** (Experimental section). The ring formation step from tetrayne **18** also afforded the expanded [4]pericyclyne **19** as the major product (as in the ethynyl-substituted version described by Diederich et al. [45]), along with small amounts of the expanded [8]pericyclyne **20** (Fig. 15). Treatment of **12** with the $SnCl_2$/HCl system successfully used for preparing first ring *carbo*-mers of benzenes **4–10**, did not allow for isolating—and even detecting—**11** under preparative conditions. In order to avoid evaporation of the solvent that was suspected to trigger decomposition, the aromatization was in situ monitored by ^{1}H NMR and UV–vis spectroscopy. Thus, adding **12** into a solution of $SnCl_2$ in a $CDCl_3$/DCl/D_2O mixture under quite diluted conditions resulted

in a turquoise blue solution (Fig. 16). NMR analysis at 278 K revealed the appearance of a set of three coupled protons at very low field. Decoupling experiments and multiplicity analysis allowed for the assignment of resonances at 10.17, 8.39, and 8.08 ppm to the ortho, meta, and para protons of the equivalent phenyl substituents at the *carbo*$_2$-benzene ring, respectively. The ring current effect is thus ca. +0.5 ppm stronger in **11** than in the lower ring-*carbo*-mer **4**, where the corresponding protons resonate at 9.45, 8.38, and 7.72 ppm, respectively. The UV–vis spectrum of the blue solution containing **11** displays an intense absorbtion band at λ_{max} = 609 nm. In comparison, diluted orange solutions of **4** give λ_{max} = 472 nm: the electron delocalization thus appear to be more extended in **11** than it is in **4**. In order to get interpretation of this feature, the structures of **4** and **11** were calculated at the B3PW91/6-31G** level. While the phenyl substituents of **4** are tilted from the planar C_{18} ring by 18.6° in average (13° in the X-ray crystal structure reported by Ueda, Kuwatani et al. [20b]), the calculated structure of **11** is perfectly planar with a D_{6h} symmetry (Fig. 16). Radial conjugation in **4** is indeed hindered by van der Waals repulsion between adjacent phenyl rings. The distance between adjacent phenyl rings is much larger in **11**, and radial conjugation from the central ring is restored. Therefore, the extended delocalization in **11**, as revealed by the UV–vis bathochromic shift, is not only due to the increased size of the central ring (C_{30}), but also to the overall planarity. This experimental shift (Δ_{exp} = 137 nm) is qualitatively reproduced by Zindo calculations (Δ_{calcd} = 107 nm).

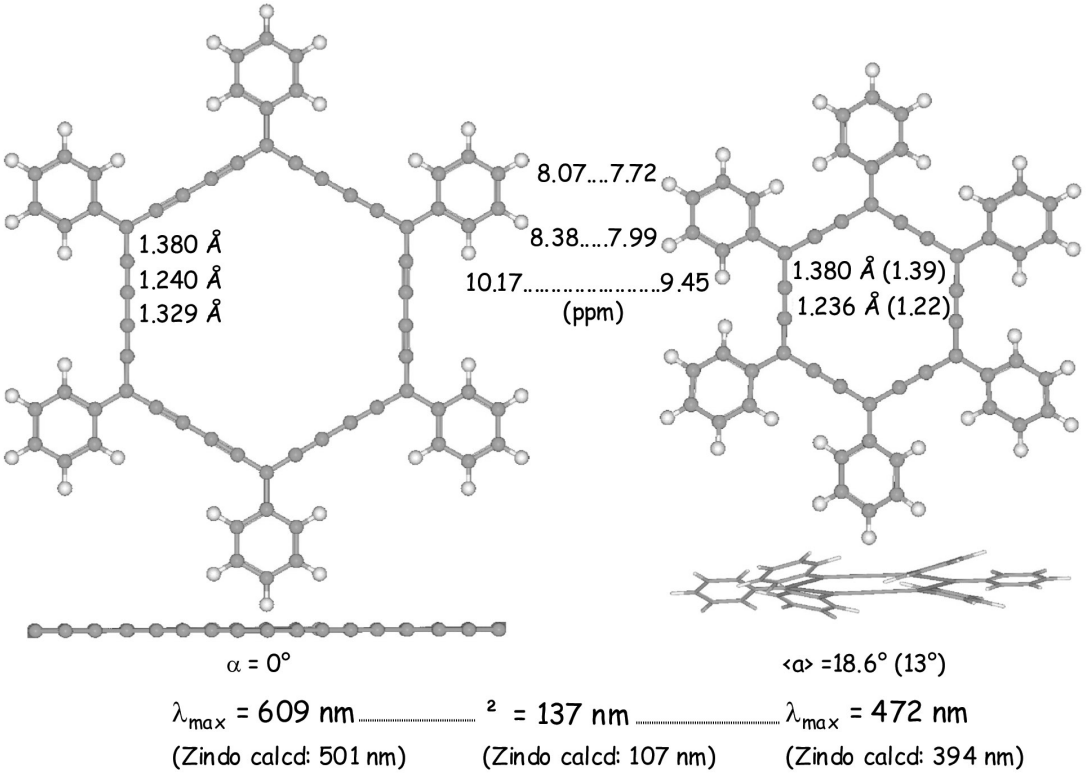

Fig. 16 Theoretical and experimental *carbo*-meric comparison of hexaphenyl-*carbo*$_k$-benzenes, k = 1, 2. Structures were calculated at the B3PW91/6-31G** level. α denotes the tilting of the phenyl planes with respect to the D_{6h} plane of the *carbo*$_k$-ring (k = 1: C_{18}; k = 2: C_{30}).

CONCLUSION

The *carbo*-mer principle proposes novel aromatic structures which are to be compared to their parent structures. It thus proposes to analyze aromaticity of cyclically unsaturated molecules vs. size and carbon content features. The wealth of the *carbo*-mer concept in the field of aromaticity has been illustrated by several representative examples, but it has been already generalized to other systems such as heterocycles [47], oxocarbons [42], fullerenes [48], and carbon nanotubes [18].

The definition also stimulates novel investigations of the aromaticity concept itself using both theoretical modeling and experimental synthesis. The first *carbo*-meric comparison between the hexaphenyl derivatives of the $carbo_2$- and $carbo_1$-benzene rings—which can be extended to the zero order through the known hexaphenylbenzene—unveils a new prospect. Synthesis of a possibly more stable $carbo_2$-benzenic molecule is currently being attempted through the hexa(*p*-anisyl)-$carbo_2$-benzene target [49]. The preliminary results give new insights into the upper threshold of the Hückel rule: The "4*n*+2" orbital occupancy criterion of aromaticity might thus remain valid up to $n = 7$ for highly symmetrical π-systems such as the $carbo_2$-benzene ring. The third *carbo*-meric generation of the benzene ring (a C_{42} ring) now deserves theoretical investigations. Finally, speculations might be extended to the fourth *carbo*-meric generation: The $carbo_4$-benzene ring (a C_{54} ring) would be the *carbo*-mer of the *carbo*-mer of benzene, and testing of the recurrent *carbo*-meric principle is at least intellectually attractive.

EXPERIMENTAL

General

All reactions were carried out under nitrogen or argon atmosphere, using Schlenk and vacuum line technics. Tetrahydrofuran (THF) and diethylether were dried and distilled over sodium/benzophenone, pentane, and dichloromethane over P_2O_5. Commercial solutions of EtMgBr and HC≡CMgBr are 3 M in diethylether and 0.5 M in THF, respectively. Commercial solutions of *n*-BuLi are 1.6 or 2.5 M in hexane, and their effective concentration were checked by titration with 2,2,2'-trimethylpropionanilide before use [50]. IR, ^1H, and ^{13}C NMR spectra were recorded in $CDCl_3$ solutions, at 250 and 62 MHz, respectively, for the latters, unless otherwise noted. IR absorption frequencies ν are in cm^{-1}. NMR chemical shifts δ are in ppm, with positive values to high frequency relative to the tetramethylsilane reference. For MS analyses, the following abreviations are adopted: DCI: desorption chemical ionization; APCI: atmospheric pressure chemical ionization; FAB: fast atom bombardment; MNBA: *m*-nitrobenzylic alcohol (matrix).

3-(Triethylsilyl)-1-phenylprop-2-yn-1-ol (13)

EtMgBr solution (8.33 mL, 25 mmol) was syringed into a solution of triethylsilylacetylene (3.543 g, 25 mmol) in THF (60 mL) at 0 °C. The mixture was stirred for 30 min at 0 °C, and then for 1 h at r.t. After cooling back to 0 °C, benzaldehyde (2.55 mL, 25 mmol) was added, and stirring was continued for 20 min at 0 °C, and then for 2.5 h at r.t. The reaction mixture was then treated with saturated aqueous NH_4Cl (60 mL) and diluted with Et_2O (20 mL). The organic layer was separated and washed with additional aqueous NH_4Cl (3×60 mL). The aqueous phases were washed with Et_2O (2×30 mL), and the combined organic phases were dried over $MgSO_4$, filtered, and concentrated under reduced pressure. Chromatography of the residue over silica gel (heptane:EtOAc 9:1) afforded **13** as a colorless oil (5.828 g, 23.65 mmol, 95 %).

MS (DCI/NH_3): *m*/*z* (%) = 264 (M+NH_4, 18), 246 (M–H_2O+NH_4, 73), 229 (M–H_2O+H, 100). ^1H NMR: $\delta = 0.63$ (q, $^3J_{HH} = 7.9$ Hz, 6H; Si$CH_2$$CH_3$), 1.01 (t, $^3J_{HH} = 7.9$ Hz, 9H; Si$CH_2$$CH_3$), 2.19 (s, br, 1H; O*H*), 5.47 (s, 1H; HO–C–*H*), 7.36 (m, 3H; *m*-, *p*-C_6H_5), 7.56 (m, 2H; *o*-C_6H_5). $^{13}C\{^1H\}$

NMR: δ = 4.15 (Si*C*H_2CH$_3$), 7.33 (SiCH$_2$*C*H$_3$), 64.71 (HO–*C*H), 88.68, (*C*≡C–Si), 106.30 (C≡*C*–Si), 126.66, 128.10, 128.35 (*m*-, *p*-, *o*-C_6H_5), 140.35 (*ipso*-C_6H_5–C). IR: ν = 3591 (m, O–H), 3068, and 3034 (w, C*sp*^{2}–H), 2958–2876 (s, C*sp*^{3}–H), 2172 (w, C≡C), 1456 (m), 1415 (m), 1038 (s), 1019 (s).

3-(Triethylsilyl)-1-phenylprop-2-yn-1-one (14)

MnO_2 powder (53.07 g, 610.5 mmol) was added to a solution of **13** (10.02 g, 40.69 mmol) in CH_2Cl (350 mL) at 0 °C. After stirring for 10 min at 0 °C and then 2.5 h at r.t., the solution was filtered through a small pad of celite, and evaporated under reduced pressure. The residue was chromatographed over silica gel (heptane:EtOAc 95:5) to give **14** as a pale yellow oil (9.73 g, 39.79 mmol, 98 %).

MS (DCI/NH_3) *m*/*z* (%): 262 (M+NH_4, 24), 245 (M+H, 100). Elemental analysis % (calcd.): C = 73.43 (73.71); H = 8.20 (8.25). ^{1}H NMR: δ = 0.71 (q, $^3J_{HH}$ = 7.9 Hz, 6H; SiCH_2Me), 1.04 (t, $^3J_{HH}$ = 7.9 Hz, 9H; SiCH$_2$CH_3), 7.51 (m, 3H; *m*-, *p*-C$_6H_5$), 8.13 (m, 2H; *o*-C$_6H_5$). ^{13}C{^{1}H} NMR: δ = 3.72 (Si*C*H$_2$Me), 7.20 (SiCH$_2$*C*H$_3$), 98.45, (*C*≡C–Si), 101.91 (C≡*C*–Si), 128.38 (*m*-C_6H_5), 129.34 (*o*-C_6H_5), 133.94 (*p*-C_6H_5), 136.36 (*ipso*-C_6H_5–C), 177.33 (*C*=O). IR: ν = 3069 (w, C*sp*^{2}–H), 2959, 2877 (s, C*sp*^{3}–H), 2151 (m, C≡C), 1640 (vs, C=O), 1599 (m), 1579 (m), 1457 (w), 1414 (w), 1450 (m), 1256 (s), 1243 (s), 1174 (m), 1039 (s), 1018 (s).

1-(Triethylsilyl)-3-phenylpenta-1,4-diyn-3-ol (15)

Ethynylmagnesium bromide (120 mL, 60 mmol) was syringed into a solution of **14** (9.78 g, 40 mmol) in THF (20 mL) at 0 °C. The mixture was stirred for 30 min at 0 °C, then overnight at r.t., and finally hydrolyzed with saturated aqueous NH_4Cl (90 mL) and diluted with Et_2O (20 mL). The phase organic layer was separated and washed with additional aqueous NH_4Cl (3 × 90 mL). The aqueous phases were extracted with Et_2O (2 × 60 mL), and the combined organic phases were dried over $MgSO_4$, filtered, and concentrated to dryness. The residue was chromatographed over silica gel (heptane:Et OAc 9:1) to provide **15** as a yellow oil (10.71 g, 39.6 mmol, 99 %).

MS (DCI/NH_3): *m*/*z* (%) = 270 (M–H_2O+NH_4, 58), 253 (M–H_2O+H, 100). ^{1}H NMR: δ = 0.68 (q, $^3J_{HH}$ = 7.9 Hz, 6H; SiCH_2Me), 1.05 (t, $^3J_{HH}$ = 7.9 Hz, 9H; SiCH$_2$CH_3), 2.76 (s, 1H; C*H*), 3.11 (s, br, 1H; OH), 7,40 (m, 3H; *m*-, *p*-C$_6H_5$), 7,85 (m, 2H; *o*-C$_6H_5$). ^{13}C{^{1}H} NMR: δ = 4.04 (Si*C*H$_2$Me), 7.30 (SiCH$_2$*C*H$_3$), 64.95 (HO–*C*), 73.15 (C≡*C*–H), 83.74 (*C*≡C–H), 87.96 (*C*≡C–Si), 105.40 (C≡*C*–Si), 125.73, 128.27, and 128.60 (*m*-, *p*-, *o*-C_6H_5), 141.12 (*ipso*-C_6H_5–C). IR: ν = 3575 (s, O–H), 3306 (s, C*sp*–H), 3088, 3065, 3032 (w, C*sp*^{2}–H), 2958-2876 (s, C*sp*^{3}–H), 2170, and 2125 (w, C≡C), 1457 (m), 1415 (m), 1450 (s), 1018 (s).

1,10-Bis(triethylsilyl)-3,8-diphenyldeca-1,4,6,9-tetrayn-3,8-diol (16)

Oxygen gas was bubbled for 15 min into a mixture of **15** (2.57 g, 9.5 mmol), TMEDA (0.11 g, 0.95 mmol) in CH_2Cl_2 (60 mL) at 0 °C. CuCl (95 mg, 0.95 mmol) was added, and the oxygen flush was maintained under stirring for 10 min at 0 °C and 3.5 h at r.t. The mixture was extracted with 20 % aqueous HCl (3 × 60 mL), then with water (30 mL) and aqueous saturated NH_4Cl (2 × 60 mL). The aqueous phases were extracted with Et_2O (2 × 60 mL), and the organic phases were combined, dried over $MgSO_4$, filtered, and concentrated to dryness. The residue was chromatographed over silica gel (heptane:EtOAc 9:1) to afford **16** as a yellow oil (2.43 g, 4.5 mmol, 95 %).

MS (DCI/NH_3): *m*/*z* (%) = 556 (M+NH_4, 1), 538 (M–H_2O+NH_4, 9), 521 (M–H_2O+H, 100). ^{1}H NMR: δ = 0.72 (q, $^3J_{HH}$ = 7.9 Hz, 12H; SiCH_2Me), 1.08 (t, $^3J_{HH}$ = 7.9 Hz, 18H; SiCH$_2$CH_3), 3.32 (s, br, 2H; O*H*), 7.42 (m, 6H; *m*-, *p*-C$_6H_5$), 7.82 (m, 4H; *o*-C$_6H_5$). ^{13}C{^{1}H} NMR: δ = 4.04 (Si*C*H$_2$Me), 7.34 (SiCH$_2$*C*H$_3$), 65.46 (HO–*C*), 68.64 (≡C–*C*≡), 80.19 (*C*≡C–C≡C), 89.00 (*C*≡C–Si), 104.39 (≡C–Si), 125.79, 128.40, and 128.82 (*m*-, *p*-, *o*-C_6H_5), 140.55 (*ipso*-C_6H_5–C). IR: ν = 3573 (s, O–H),

3066 and 3031 (w, Csp^2–H), 2958-2876 (s, Csp^3–H), 2156 (w, C≡C), 1457 (m), 1415 (m), 1450 (s), 1018 (s).

3,8-Diphenyldeca-1,4,6,9-tetrayn-3,8-diol (17)

A solution of **16** (3.72 g, 6.90 mmol) in THF (60 mL) was poured into a mixture of K_2CO_3 (1.91 g, 13.8 mmol) in methanol (60 mL) at r.t. After stirring overnight, the mixture was concentrated under reduced pressure and rediluted with Et_2O (100 mL) and water (100 mL). The organic phase was separated and washed with saturated aqueous NH_4Cl (3 × 60 mL). The aqueous phases were in turn washed with Et_2O (2 × 60 mL), and the combined organic layers were dried over $MgSO_4$, filtered, and concentrated to dryness. Chromatography of the residue over silica gel (heptane:EtOAc 7:3) afforded **17** as a yellow powder (1.97 g, 6.35 mmol, 92 %).

MS (DCI/NH_3): *m/z* (%) = 345 (M+N_2H_7, 2), 328 (M+NH_4, 13), 310 (M–H_2O+NH_4, 83), 293 (M–H_2O+H, 100). ^{1}H NMR: δ = 2.82 (s, 2H; ≡CH), 3,05 (s, br, 2H; O*H*), 7.39 (m, 6H; *m*-, *p*-C_6H_5), 7.75 (m, 4H; *o*-C_6H_5). ^{13}C{^{1}H} NMR: δ = 64.97 (HO-*C*), 68.70 (C≡*C*–C≡C), 74.38 (C≡*C*–H), 79.74 (*C*≡C–C≡*C*), 82.16 (*C*≡C–H), 125.56, 128.51, 129.05 (*m*-, *p*-, *o*-C_6H_5), 139,81 (*ipso*-C_6H_5–C). IR: ν = 572 (s, O–H), 3304 (s, C*sp*–H), 3089, 3068, and 3032 (w, Csp^2–H), 2157, and 2124 (w, C≡C), 1490 (s), 1450 (s), 1029 (s). UV ($CHCl_3$): λ_{max} (nm) (lgε) = 289 (1.96). Mp: starts at 99 °C. Selective crystallization from EtOAc afforded white plates of the *meso*-isomer of **17**, as established by X-ray diffraction analysis.

3,8-Dimethoxy-3,8-diphenyldeca-1,4,6,9-tetrayne (18)

n-Butyllithium solution (2.5 M, 4.84 mL, 12.1 mmol) was syringed into a solution of **17** (1.91 g, 6.15 mmol) in THF (50 mL) at –78 °C. After stirring for 30 min, iodomethane (3.80 mL, 61.5 mmol) and DMSO (4.10 mL, 61.5 mmol) were added, and the temperature was allowed to warm up to r.t. The mixture was stirred overnight at r.t. and then diluted with Et_2O (20 mL) and water (60 mL). The organic layer was separated and washed with saturate aqueous NH_4Cl (3 × 60 mL). The aqueous phases were extracted with Et_2O (2 × 30 mL). The combined organic phases were dried over $MgSO_4$, filtered, and concentrated to dryness. Chromatography of the residue over silica gel (heptane:EtOAc 8:2) afforded **18** as a sticky brown solid (1.90 g, 5.62 mmol, 91 %).

MS (DCI/NH_3): *m/z* (%) = 356 (M+NH_4, 0.4), 338 (M–H_2O+NH_4, 0.8), 307 (M–MeOH+H, 100). ^{1}H NMR: δ = 2.82 (s, 2H; ≡C*H*), 3.55 (s, 6H; OCH_3), 7.40 (m, 6H; *m*-, *p*-C_6H_5), 7.74 (m, 4H; *o*-C_6H_5). ^{13}C{^{1}H} NMR: δ = 53.57 (O*C*H_3), 70.22 (*C*-OMe), 71.94 (C≡*C*–*C*≡C), 76.10 (C≡*C*–H), 77.79 (*C*≡C–C≡*C*), 79,83 (*C*≡CH), 126.42, 128.60, 129.23 (*m*-, *p*-, *o*-C_6H_5), 139.03 (*ipso*-C_6H_5–C). IR: ν = 3304 (s, C*sp*–H), 3066 and 3031 (w, Csp^2–H), 3001-2828 (w, Csp^3–H), 2154 and 2121 (w, C≡C), 1490 (m), 1450 (s), 1060 (vs).

1,6,11,16-Tetramethoxy-1,6,11,16-tetraphenylcycloeicosa-2,4,7,9,12,14,17,19-octayne (19), 1,6,11,16,21,26-hexamethoxy-1,6,11,16,21,26-hexaphenylcyclotriaconta-2,4,7,9,12,14,17,19,22,24,27,29-dodecayne (12), and 1,6,11,16,21,26,31,36-octamethoxy-1,6,11,16,21,26,31,36-octaphenylcyclotetraconta-2,4,7,9, 12,14,17,19,22,24,27,29,32,34,37,39-hexadecayne (20)

To a solution of **18** (0.56 g, 1.66 mmol) in a 1:1 mixture of DMF and pyridine (200 mL) was added $Cu(OAc)_2$ (4.81 g, 26.5 mmol) and CuCl (1.97 g, 19.9 mmol). The mixture was stirred for 16 h at r.t., then for 48 h at 60–65 °C, and finally concentrated under reduced pressure at 60 °C and diluted with chloroform (60 mL). After extraction with 20 % aqueous HCl (3 × 60 mL) and saturated aqueous NH_4Cl (2 × 60 mL), the aqueous phases were washed with Et_2O (2 × 60 mL), and the combined or-

ganic phases were dried over $MgSO_4$, filtered, and evaporated to dryness. The residue was chromatographed over silica gel (pentane:Et_2O 7:3). Primary separation products were submitted to further chromatographies to finally give three samples of white powders corresponding to the expanded pericyclynes **19** (276 mg, 0.41 mmol, 49 %), **12** (84 mg, 0.083 mmol, 15 %), and **20** (20 mg, 0.015 mmol, 4 %).

Analytical data for **19**. TLC (SiO_2, pentane:Et_2O 6:4): $R_f \approx 0.38$. MS (FAB, MNBA): *m*/*z* (%) = 695 (M+Na), 641 (M–OMe). ^{1}H NMR: δ = 3.60 (m, 12H; OCH_3), 7.41 (m, 12H; *m*-, *p*-C_6H_5), 7.69 (m, 8H; *o*-C_6H_5). ^{13}C{^{1}H} NMR: δ = 54.08 (OCH_3), 72.01 and 72.12 (MeO–*C*), 72.92 (C≡*C*–*C*≡C), 79.63, 79.80, 79.85 (*C*≡C–C≡*C*), 126.45, 128.74, 129.51 (*m*-, *p*-, *o*-C_6H_5), 137.77 (*ipso*-C_6H_5-C). IR: ν = 3065 and 3030 (w, Csp^2–H), 2959-2829 (m, Csp^3–H), 2149 (m, C≡C), 1490 (m), 1461 (m), 1451 (s), 1174 (m), 1070 (s), 1015 (s). UV ($CHCl_3$): λ_{max} = 241 nm. Mp = 138 °C (dec.).

Analytical data for **12**. TLC (SiO_2, pentane:Et_2O 6:4): $R_f \approx 0.26$. MS [APCI, $CHCl_3$ (CH_3CN-Ac.form. 0.5 %/50-50)]: *m*/*z* (%) = 1018.8 (M–OMe+CH_3CN), 1009.8 (M+H), 986.8 (M–MeOH–OMe+CH_3CN), 977.5 (M–OMe), 945.7 (M–MeOH–OMe), 913.7 (M–2MeOH–OMe). ^{1}H NMR: δ = 3.62 (m, 18H; OCH_3), 7.43 (m, 18H; *m*-, *p*-C_6H_5), 7.74 (m, 12H; *o*-C_6H_5). ^{13}C{^{1}H} NMR: δ = 53.83 (OCH_3), 70.81 (MeO–*C*), 72.31 (C≡*C*–*C*≡C), 76.95 (*C*≡C–C≡*C*), 126.22, 128.56, 129.28 (*m*-, *p*-, *o*-C_6H_5), 138.29 (*ipso*-C_6H_5–C). IR: ν = 3065 and 3030 (w, Csp^2–H), 2959-2829 (m, Csp^3–H), 2152 (m, C≡C), 1490 (s), 1461 (m), 1450 (s), 1172 (s), 1069 (s), 1038 (s), 1027 (s). UV ($CHCl_3$): λ_{max} (approximate absorbance) = 241 nm (1.11), 268 nm (shoulder, 0.34).

Analytical data for **20**. TLC (SiO_2, pentane:Et_2O 6:4): $R_f \approx 0.19$. MS [APCI, $CHCl_3$ (CH_3CN-Ac. form. 0.5 %/50-50)]: *m*/*z* (%) = 1346.8 (M+H), 1314.1 (M–OMe), 1281.8 (M–MeOH–OMe), 1250.9 (M–2MeOH–OMe). ^{1}H NMR: δ = 3.58 (m, 24H; OCH_3), 7.39 (m, 24H; *m*-, *p*-C_6H_5), 7.70 (m, 16H; *o*-C_6H_5). ^{13}C{^{1}H} NMR: δ = 53.94 (OCH_3), 70.97 (MeO–*C*), 72.48 (C≡*C*–*C*≡C), 77.11 (*C*≡C–C≡*C*), 126.35, 128.69, 129.41 (*m*-, *p*-, *o*-C_6H_5), 138.45 (*ipso*-C_6H_5-C). IR: ν = 3066 and 3031 (w, Csp^2–H), 2959-2829 (m, Csp^3–H), 2151 (m, C≡C), 1490 (m), 1461 (m), 1450 (s), 1173 (m), 1068 (s), 1045 (s), 1029 (m).

5,10,15,20,25,30-Hexaphenyl-1,2,3,4,6,7,8,9,11,12,13,14,16,17,18,19,21,22,23,24,26,27,28,29-tetraicosadehydro[30]annulene (11)

In an NMR tube, $SnCl_2$ (ca. 3 mg, 1.6 10^{-2} mmol) was dissolved in a biphasic mixture of a 20 % DCl solution in D_2O (ca. 0.25 mL) and $CDCl_3$ (ca. 0.5 mL). A solution of **12** (ca. 0.5 mg, 5.10^{-4} mmol) in $CDCl_3$ (0.5 mL) was added. After vigorous shaking for 10 min at 20 °C, the diluted organic phase turned to turquoise blue (samples at higher concentrations were blue–violet). The chloroform phase was cooled to 278 K and analyzed by ^{1}H NMR spectroscopy at 500 MHz. The UV spectrum of the solution was then recorded at r.t. (Fig. 13).

^{1}H NMR (500 MHz, $CDCl_3$): δ = 8.08 (m, 6H; *p*-C_6H_5), 8.39 (t, $^3J_{HH}$ = 5 Hz, 12H; *p*-C_6H_5), 10.17 (d, $^3J_{HH}$ = 5 Hz, 12H; *o*-C_6H_5). UV ($CDCl_3$): λ (nm) (approximate absorbance) = 517 (0.3), 546 (0.3), 609 (0.8), 653 (shoulder, 0.3), 672 (0.4).

REFERENCES

1. P. Hohenberg, W. Kohn. *Phys. Rev. B* **136**, 864 (1964).
2. R. F. W. Bader, P. L. A. Popelier, T. A. Keith. *Chem. Rev.* **91**, 893 (1991).
3. (a) E. Ruch. *Acc. Chem. Res.* **5**, 49 (1972); (b) A. Rassat. *C. R. Acad. Sci., Ser. II* **199**, 53 (1984); (c) A. B. Buda, K. Mislow. *J. Am. Chem. Soc.* **114**, 6006 (1992); (d) R. Chauvin. *J. Phys. Chem.* **96**, 4706 (1992); (e) H. Zabrodsky, D. Avnir. *J. Am. Chem. Soc.* **117**, 462 (1995); (f) R. Chauvin. *J. Math. Chem.* **19**, 147 (1996); (g) P. Legennec. *J. Math. Phys.* **41**, 5954 (2000); (h) M. Petitjean. *Entropy* **5**, 271 (2003).

4. (a) V. E. Minkin, M. N. Glukhotsev, B. Y. A. Simkin. In *Aromaticity and Antiaromaticity. Electronic and Structural Aspects*, John Wiley, New York (1994); (b) M. K. Cyrañski. *Chem. Rev.* **105**, 3773 (2005).
5. A. R. Katritsky, P. Barczynski, G. Musumarra, D. Pisano, M. Szafran. *J. Am. Chem. Soc*. **111**, 7 (1989).
6. T. M. Krygowski, M. K. Cyrañski. *Chem. Rev.* **101**, 1395 (2001).
7. P. v. R. Schleyer, C. Maerker, A. Dransfeld, H. Jiao, N. J. R. v. E. Hommes. *J. Am. Chem. Soc.* **118**, 6317 (1996).
8. (a) P. Lazzeretti. *Progr. Magn. Res. Spectr.* **36**, 1 (2000); (b) J. A. N. Gomes, R. B. Mallion. *Chem. Rev.* **101**, 1349 (2001).
9. J. Pipek, P. G. Mezey. *J. Phys. Chem.* **90**, 4916 (1989).
10. B. Silvi, A. Savin. *Nature* **371**, 683 (1994).
11. P. v. R. Schleyer, P. K. Freeman, H. Jiao, B. Goldfuss. *Angew. Chem., Int. Ed. Engl.* **34**, 337 (1995).
12. (a) R. Chauvin. *Tetrahedron Lett.* **36**, 397 (1995); (b) R. Chauvin. *Tetrahedron Lett.* **36**, 401 (1995).
13. H. Jiao, N. J. R. van E. Hommes, P. v. R. Schleyer, A. de Meijere. *J. Org. Chem.* **61**, 2826 (1996).
14. (a) L. T. Scott, G. J. DeCicco, J. L. Hyun, G. Reinhardt. *J. Am. Chem. Soc.* **105**, 7760 (1983); (b) L. T. Scott, G. J. DeCicco, J. L. Hyun, G. Reinhardt. *J. Am. Chem. Soc.* **107**, 6546 (1985); (c) K. N. Houk, L. T. Scott, N. G. Rondan, D. C. Spellmeyer, G. Reinhardt, J. L. Hyun, G. J. DeCicco, R. Weiss, M. H. M. Chen, L. S. Bass, J. Clardy, F. S. Jorgensen, T. A. Eaton, V. Sarkozi, C. M. Petit, L. Ng, K. D. Jordan. *J. Am. Chem. Soc.* **107**, 6556 (1985).
15. C. Lepetit, B. Silvi, R. Chauvin. *J. Phys. Chem. A* **107**, 464 (2003).
16. (a) L. Maurette, C. Godard, S. Frau, C. Lepetit, M. Soleilhavoup, R. Chauvin. *Chem. Eur. J.* **7**, 1165 (2001); (b) L. Maurette, C. Tedeschi, E. Sermot, M. Soleilhavoup, F. Hussain, B. Donnadieu, R. Chauvin. *Tetrahedron* **60**, 10077 (2004).
17. C. Saccavini, L. Maurette, C. Tedeschi, C. Sui-Seng, S. Soula, M. Soleilhavoup, L. Vendier, C. Zou, R. Chauvin. Manuscript in preparation.
18. C. Lepetit, C. Zou, R. Chauvin. Submitted for publication.
19. C. Saccavini, C. Sui-Seng, L. Maurette, B. Donnadieu, C. Lepetit, R. Chauvin. Manuscript in preparation.
20. (a) Y. Kuwatani, N. Watanabe, I. Ueda. *Tetrahedron Lett.* **36**, 119 (1995); (b) R. Suzuki, H. Tsukuda, N. Watanabe, Y. Kuwatani, I. Ueda. *Tetrahedron* **54**, 2477 (1998).
21. K. Nakatani, P. G. Lacroix, C. Saccavini, R. Chauvin. Unpublished results.
22. C. Lepetit, P. G. Lacroix, V. Peyrou, C. Saccavini, R. Chauvin. *J. Comput. Met. Sci. Eng*. **4**, 569 (2004).
23. R. Chauvin, C. Lepetit. In *Acetylene Chemistry*, F. Diederich, P. J. Stang, R. R. Tykwinski (Eds.), pp. 1–50, VCH, Weinheim (2005).
24. A. Soncini, P. W. Fowler, I. Cernusak, E. Steiner. *Phys. Chem. Chem. Phys.* **3**, 3920 (2001).
25. J. C. Santos, W. Tiznado, R. Contreras, P. Fuentealba. *J. Chem. Phys.* **120**, 1670 (2004).
26. R. S. Mulliken, R. G. Parr. *J. Chem. Phys.* **19**, 1271 (1951).
27. W. J. Hehre, R. Dichtfield, L. Radom, J. A. Pople. *J. Am. Chem. Soc.* **92**, 4796 (1970).
28. P. Georges, M. Trachtman, C. W. Bock, A. M. Brett. *Tetrahedron* **32**, 317 (1976).
29. B. A. Hess Jr., L. J. Schaad. *J. Am. Chem. Soc.* **105**, 7500 (1983).
30. H. Jiao, P. v. R. Schleyer. *Angew. Chem., Int. Ed. Engl.* **35**, 2383 (1996).
31. S. Shaik, P. C. Hiberty, J.-M. Lefour, G. Ohanessian. *J. Am. Chem. Soc.* **109**, 363 (1987).
32. (a) R. Breslow, E. Mohacsi. *J. Am. Chem. Soc.* **85**, 431 (1963); (b) J. Aihara, H. Ichikawa. *Bull. Chem. Soc.* **61**, 223 (1988).
33. R. C. Haddon. *J. Am. Chem. Soc.* **101**, 1722 (1979).

34. C. Lepetit, C. Godard, R. Chauvin. *New J. Chem.* **25**, 572 (2001).
35. C. Godard, C. Lepetit, R. Chauvin. *Chem. Commun.* 1833 (2000).
36. M. B. Nielsen, M. Schreiber, Y. G. Baek, P. Seiler, S. Lecomte, C. Boudon, R. R. Tykwinski, J.-P. Gisselbrecht, V. Gramlich, P. J. Skinner, C. Bosshard, P. Günter, M. Gross, F. Diederich. *Chem. Eur. J.* **7**, 3263 (2001).
37. C. Lepetit, M. B. Nielsen, F. Diederich, R. Chauvin. *Chem. Eur. J.* **9**, 5056 (2003).
38. (a) Y. Tobe, R. Umeda, N. Iwasa, M. Sonoda. *Chem. Eur. J.* **9**, 5549 (2003); (b) M. Iyoda, Y. Kuwatani, S. Yamagata, N. Nakamura, M. Todaka, G. Yamamoto. *Org. Lett.* **6**, 4667 (2004).
39. M. Gholami, R. R. Tykwinski. *11th International Symposium on Novel Aromatic Compounds*, Abstract 288 (2005).
40. B. Ma, H. M. Sulzbach, Y. Xie, F. H. Schaefer III. *J. Am. Chem. Soc.* **116**, 3529 (1994).
41. (a) H. Hopf, G. Maas. *Angew. Chem., Int. Ed. Engl.* **31**, 931 (1992); (b) D. W. Rogers, F. J. McLafferty. *J. Phys. Chem. A* **106**, 1054 (2002).
42. M. Gicquel, C. Lepetit, J.-L. Heully, R. Chauvin. *Chimia* **59**, 448, P206 (2005).
43. See, for example: A. de Meijere, S. Kozhushkov. *Chem. Eur. J.* **8**, 3195 (2002) and refs. therein.
44. (a) M. Brake, V. Enkelmann, U. H. F. Bunz. *J. Org. Chem.* **61**, 1190 (1996); (b) B. Leibrock, O. Vostrowsky, A. Hirsch. *Eur. J. Org. Chem.* 4401 (2001); (c) F. Toda, J. Okada, K. Mori. *Angew. Chem., Int. Ed. Engl.* **27**, 859 (1988).
45. P. Manini, W. Amrein, V. Gramlich, F. Diederich. *Angew. Chem., Int. Ed.* **41**, 4339 (2002).
46. For an example, see: Y.-L. Zhao, Q. Liu, J.-P. Zhang, Z.-Q. Liu. *J. Org. Chem.* **70**, 6913 (2005) and refs. therein.
47. C. Lepetit, V. Peyrou, R. Chauvin. *Phys. Chem. Chem. Phys*. **6**, 303 (2004).
48. P. D. Jarowski, F. Diederich, K. N. Houk. *J. Org. Chem.* **70**, 1671 (2005).
49. C. Zou, R. Chauvin. Work in progress.
50. J. Suffert. *J. Org. Chem.* **54**, 509 (1989).